THE JOURNAL OF PHYSICAL CHEMISTRY B

Article

Cite This: J. Phys. Chem. B XXXX, XXX, XXX−XXX

pubs.acs.org/JPCB

A Quantitatively Accurate Theory To Predict Adsorbed Configurations of Linear Surfactants on Polar Surfaces

Sumit Sharma,* Himanshu Singh, and Xueying Ko

Department of Chemical and Biomolecular Engineering, Ohio University, Athens, Ohio 45701, United States

Supporting Information

ABSTRACT: Surfactant molecules are known to adsorb onto polar surfaces in different morphologies. The ability to predict the adsorption morphologies is important for tuning interfacial properties via surfactant adsorption. Linear surfactant molecules may adsorb in a stripe-like configuration (stripes) with their molecular axes parallel to the surface and to one another or as a self-assembled monolayer (SAM) with the molecular axes perpendicular to the surface. By comparing the associated energetics of these configurations, the favorable one can be predicted. Based on this concept, we have developed a theoretical model with no fitting parameters for describing adsorbed configurations of linear surfactant molecules on polar surfaces. The predictions of the model are in excellent agreement with the results of molecular simulations. In addition, our model explains observations of different kinetic pathways for SAM formation, which have been reported in experiments.

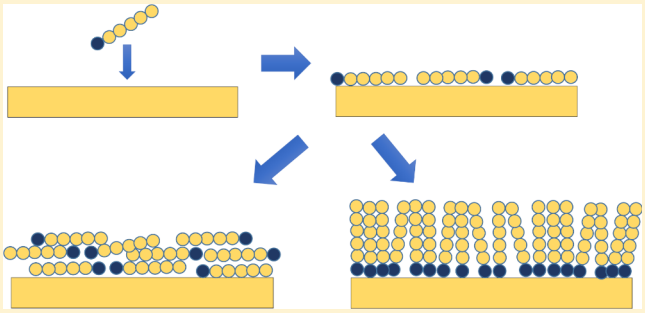

1. INTRODUCTION

Adsorption of surfactants on polar surfaces has numerous applications, including in corrosion inhibition,[1] electrochemical reactions,[2] synthesis of anisotropic metal nanoparticles,[3] and heterogeneous catalysis.[4] Surfactants are known to adsorb onto polar surfaces in various morphologies, such as (hemi-) cylinders, (hemi-) spheres, or planar micelles.[5,6] Morphology of adsorbed surfactant films is an important determinant of interfacial properties.[7,8] An ingenious thermodynamics-based theory for predicting adsorbed morphologies of surfactants on hydrophobic and hydrophilic surfaces was introduced by Johnson and Nagarajan.[9,10] However, it was not widely adopted because its predictions for hydrophilic surfaces did not match atomic force microscopy results and it required thermodynamic parameters like chemical potential of surfactants in different aggregation states, which are not easily obtainable from experiments or computer simulations.

Linear surfactant molecules, that is, molecules with a linear alkyl tail and a polar head group commensurate in size with an alkyl group, may adsorb as stripes with their molecular axes parallel to the surface and to each other[11,12] or as a self-assembled monolayer (SAM) with their molecular axes perpendicular to the surface.[13,14] However, there is no theoretical formalism for a priori predicting which configuration will be favored. Furthermore, experiments have revealed different kinetic pathways associated with the formation of a SAM of adsorbed surfactants on polar substrates like mica and gold. For instance, adsorption of octadecylphosphonic acid[15,16] and octadecyltrimethyl ammonium bromide (C_{18}TAB)[13] on mica initiates with nucleation of densely packed molecular islands followed by growth and coalescence of these islands into a contiguous adsorbed monolayer.[15,16] The adsorption and self-assembly of alkanethiols on gold follow a different kinetic pathway. It comprises two steps: in the first step, the molecules completely cover the gold surface by adsorbing parallel to the surface in the form of stripes. The second step involves an orientational transition wherein the molecules "stand up" on the surface with their molecular axes parallel to the surface normal.[17] A similar orientational transition has been reported in other studies of alkanethiols on gold.[18] So far, there exists no theoretical basis to predict when one pathway is favored over the other.

In this work, we introduce a mathematical model to predict adsorbed configurations of linear surfactants on polar surfaces. From molecular simulations, we show that our model's predictions are quantitatively accurate without the need of any fitting parameters. The model is based on the idea that linear surfactant molecules in the lying-down configuration maximize their interactions with the surface but also occupy a larger surface area. The standing-up configuration, on the other hand, allows more molecules to adsorb on the surface. In the lying-down configuration, the molecules optimize their intermolecular interactions to eventually form a stripe morphology, while the standing-up configuration ultimately results in a SAM. Based on our theory, the kinetics associated with the formation of a SAM can also be predicted. The details of our theoretical model are discussed below.

Received: June 19, 2019
Revised: July 31, 2019
Published: August 6, 2019

DOI: 10.1021/acs.jpcb.9b05861
J. Phys. Chem. B XXXX, XXX, XXX−XXX

2. THEORETICAL MODEL

Consider a surfactant molecule with a polar head group and an n carbon long alkyl tail. When these surfactant molecules are lying flat on a solid surface, the total interaction energy is given by

$$E^{L} = (\varepsilon_{HS}^{L} + n\varepsilon_{TS}^{L})\frac{A}{A_{m}^{L}}P^{L} \quad (1)$$

where the superscript L indicates the lying-down configuration, ε_{HS} is the interaction strength of the polar head with the surface, ε_{TS} is the interaction strength of a tail group with the surface, A is the total adsorption surface area, A_m is the area occupied by one surfactant molecule, and P is the packing fraction of the molecules adsorbed on the surface. In the standing-up configuration, the total interaction energy is given by

$$E^{S} = \varepsilon_{HS}^{S}\frac{A}{A_{m}^{S}}P^{S} \quad (2)$$

The superscript S indicates the standing-up configuration. Equations 1 and 2 are applicable to surfactant molecules of any geometry. P^S can be estimated as $P^S = N\frac{A_m^S}{A}$, where N is the number of molecules adsorbed in the standing-up configuration. For a linear surfactant molecule, approximated as a cylinder, $A_m^L = ld$, $A_m^S = \frac{\pi d^2}{4}$, and $P^L \approx 1$, where l is the length and d is the diameter of the cylinder. Furthermore, if the interactions of the polar head and the tail groups are isotropic, that is, they do not depend on the adsorbed configuration, then the subscripts L and S from the interaction terms may be dropped. The ratio of eqs 1 and 2 thus becomes

$$\frac{E^{L}}{E^{S}} = \frac{\pi d}{4lP^{S}}\left(1 + \frac{n\varepsilon_{TS}}{\varepsilon_{HS}}\right) \quad (3)$$

If the ratio $\frac{E^L}{E^S} < 1$, standing-up configurations are favored, which will eventually lead to formation of a SAM.

3. SIMULATION SYSTEM AND METHODS

To test the validity of the theory, we have performed Langevin dynamics simulations to determine adsorbed configurations of linear surfactant molecules with different values of ε_{TS} and ε_{HS} on a polar solid surface. Surfactant molecules are modeled as linear bead-spring chains, same as in our previous study.[19] The first bead of the molecules represents the polar head group, and the remaining ones represent the alkyl tail. We have studied surfactant molecules comprising 20 beads. The interactions of the surface with the polar head and the tail beads are modeled via 9-3 potential, which is the potential function obtained when the Lennard-Jones (LJ) potential is integrated over a semi-infinite slab. The solvent is treated implicitly in these simulations. All quantities in the simulation system are in reduced units.[20] In these units, the thermal energy k_BT is taken as the unit of energy, and thus, $k_BT = 1$. The interaction between any two tail beads is modeled via the LJ potential with $\varepsilon_{TT} = 0.065$ and $\sigma = 1$. This value of ε_{TT} results in formation of a SAM for the case when there is no interaction between the alkyl tail and the surface, that is $\varepsilon_{TS} = 0$.[19] The overall hydrophobic interaction between two alkyl tails is of the order of k_BT.[21] The magnitude of ε_{HS} matches binding energies between polar groups and metals determined from the density functional theory.[22] With σ taken as the unit of length in reduced units, the equilibrium bond length between adjacent beads is 0.3. The mass of each bead m is set to 1. In the Langevin dynamics simulations, the time step and the damping parameter are chosen to be 0.001 $\sigma(m/k_BT)^{1/2}$ and 0.1 $\sigma(m/k_BT)^{1/2}$, respectively. The force constants for bond and angle harmonic potentials are 100 k_BT/σ^2 and 50 k_BT/radians^2, respectively. These model parameters of surfactants are taken from our previous study.[19] The simulation box is periodic in the $x-y$ directions, and the polar surface is at $z = 0$. The opposite face of the simulation box has an athermal surface with reflective boundary conditions for all beads. The size of the simulation box is 20 × 20 × 40. The simulation system has 400 surfactant molecules. The initial configuration is generated by placing the surfactant molecules randomly in the simulation box. We have confirmed the invariability of our simulation results in a larger system (800 molecules with simulation box size 20 × 20 × 80) for some data points.

Our previous work[23] on atomistic simulations of surfactants in bulk and near metal surfaces has shown that (a) surfactant molecules form micelles with polar groups on the outside and alkyl tails in the core, implying that the alkyl tails have only weak interactions with the polar groups and (b) in infinite dilution, the surfactant molecules adsorb with their alkyl tail lying parallel to the metal surface, suggesting that the tails have net attractive interactions with the surface. Thus, in our coarse-grained model, only excluded volume interactions between the polar heads and the alkyl tails have been considered, while the interactions between the alkyl tails and the surface are attractive.

4. RESULTS AND DISCUSSION

4.1. Validating the Theoretical Model. Figure 1 shows results of equilibrated adsorbed configurations of surfactant molecules obtained from Langevin dynamics simulations. Each data point in Figure 1 is from a Langevin dynamics simulation with a specific set of (ε_{TS}, ε_{HS}) parameters. The theoretical line of $E^L = E^S$ calculated from eq 3 is also shown. In eq 3 for 20-mer surfactants, $l = 6$ and $d = 1$. P^S is calculated as $P^S = \frac{N\pi d^2}{4A}$, where N is the number of adsorbed molecules in the SAM. For a surface area of 20 × 20, $N \approx 310$, which gives $P^S = 0.6$.

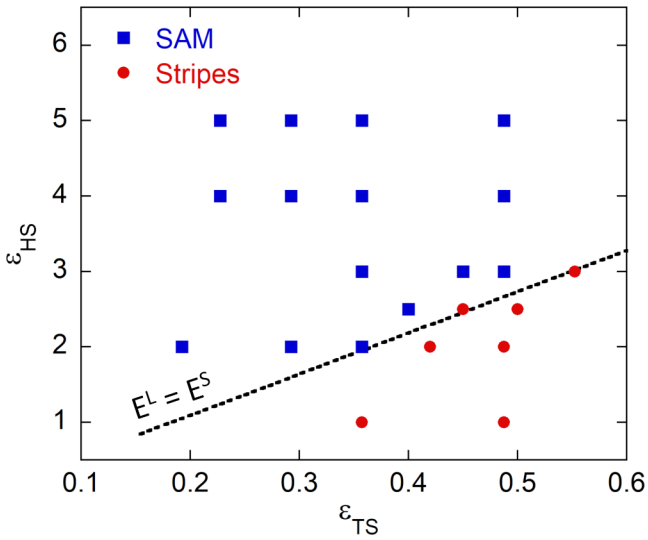

Figure 1. Summary of results of Langevin dynamics simulations performed for different values of (ε_{TS}, ε_{HS}). The dashed line shows the condition when $E^L = E^S$. An excellent match between the simulation results and theoretical predictions is obtained.

DOI: 10.1021/acs.jpcb.9b05861
J. Phys. Chem. B XXXX, XXX, XXX−XXX

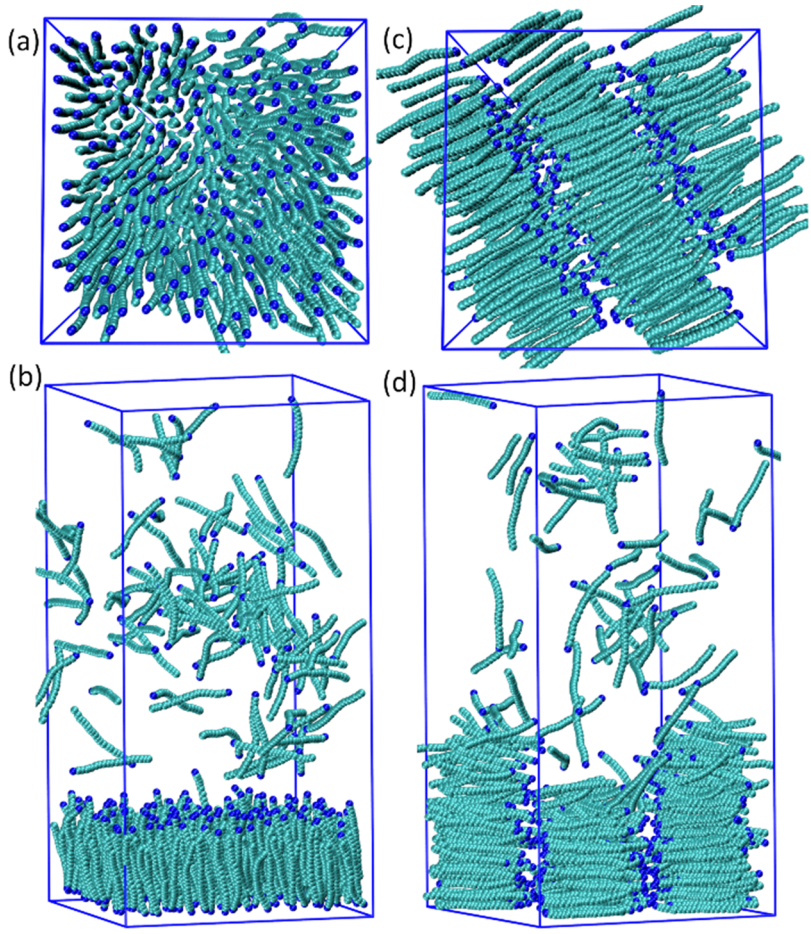

Figure 2. Snapshots of equilibrium configurations: (a) bottom view and (b) side view for $(\varepsilon_{TS}, \varepsilon_{HS}) = (0.49, 3.0)$ showing SAM and (c) bottom view and (d) side view for $(\varepsilon_{TS}, \varepsilon_{HS}) = (0.55, 3.0)$ showing stripes.

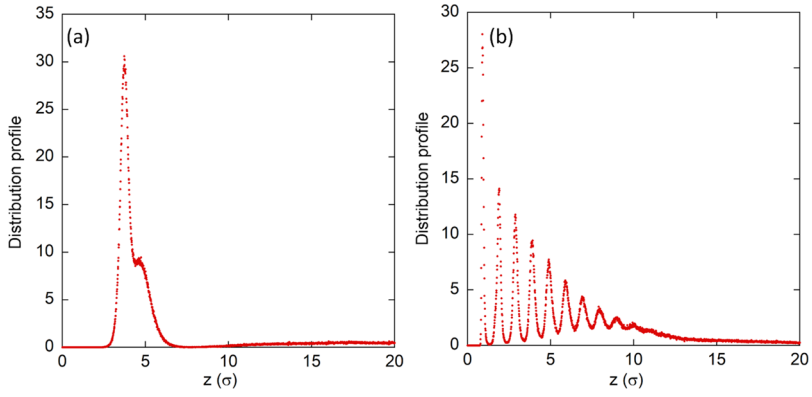

Figure 3. Equilibrium distribution of surfactant molecules as a function of distance from the surface z for (a) $(\varepsilon_{TS}, \varepsilon_{HS}) = (0.49, 3.0)$ and (b) $(\varepsilon_{TS}, \varepsilon_{HS}) = (0.55, 3.0)$. The distribution in panel (a) shows a monolayer of adsorbed molecules standing-up on the surface with a partially formed second layer appearing as a shoulder. The distribution in panel (b) shows multilayer adsorption of surfactant molecules lying down on the surface.

As per the model, when the ε_{HS} is larger in magnitude (that is, more attractive) than the value corresponding to the $E^L = E^S$ line for a given ε_{TS}, the equilibrium configuration is expected to be a SAM, while below the $E^L = E^S$ line, it is expected to be stripes. The simulation results are found to be in excellent agreement with the theoretical predictions implying that our theoretical model is quantitatively accurate. Figure 2 shows snapshots of two different state points. Figure 2a,b corresponds to $(\varepsilon_{TS}, \varepsilon_{HS}) = (0.49, 3.0)$, and Figure 2c,d corresponds to $(\varepsilon_{TS}, \varepsilon_{HS}) = (0.55, 3.0)$. For $(\varepsilon_{TS}, \varepsilon_{HS}) = (0.49, 3.0)$, a SAM configuration is obtained, while for $(\varepsilon_{TS}, \varepsilon_{HS}) = (0.55, 3.0)$, a stripe configuration is obtained. In the stripe configuration, the molecules stack up in multiple layers. The bottom view of the stripe configuration shows that the molecules are arranged in linear, parallel stripes. In the SAM configuration, the molecules stand up on the surface and are parallel to each other. In Figure 3, the density distribution of surfactant molecules is plotted as a function of the distance z from the surface for these two equilibrium configurations. Figure 3a shows that the SAM configuration is predominantly a monolayer with a shoulder due to the

DOI: 10.1021/acs.jpcb.9b05861
J. Phys. Chem. B XXXX, XXX, XXX−XXX

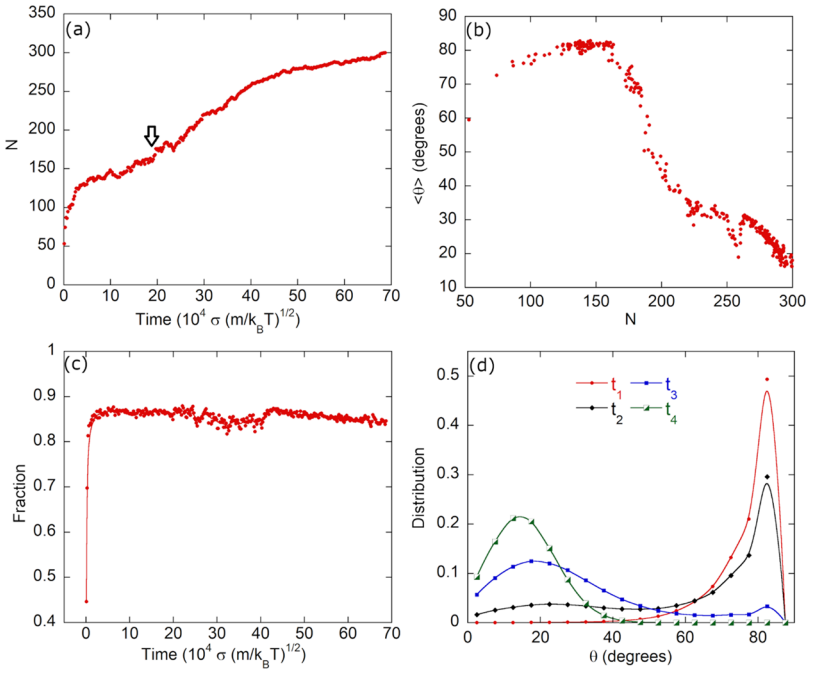

Figure 4. A simulation trajectory with $(\varepsilon_{TS}, \varepsilon_{HS}) = (0.49, 3.0)$. (a) Total number of adsorbed molecules, N as a function of time. (b) Average angle that the axes of adsorbed molecules make with the surface normal $\langle\theta\rangle$ as a function of N. (c) Fraction of the surface covered with the adsorbed molecules, *Fraction* as a function of time. (d) Distribution of angles, θ that adsorbed molecules make with the surface normal for different time periods ($t_4 > t_3 > t_2 > t_1$, see text).

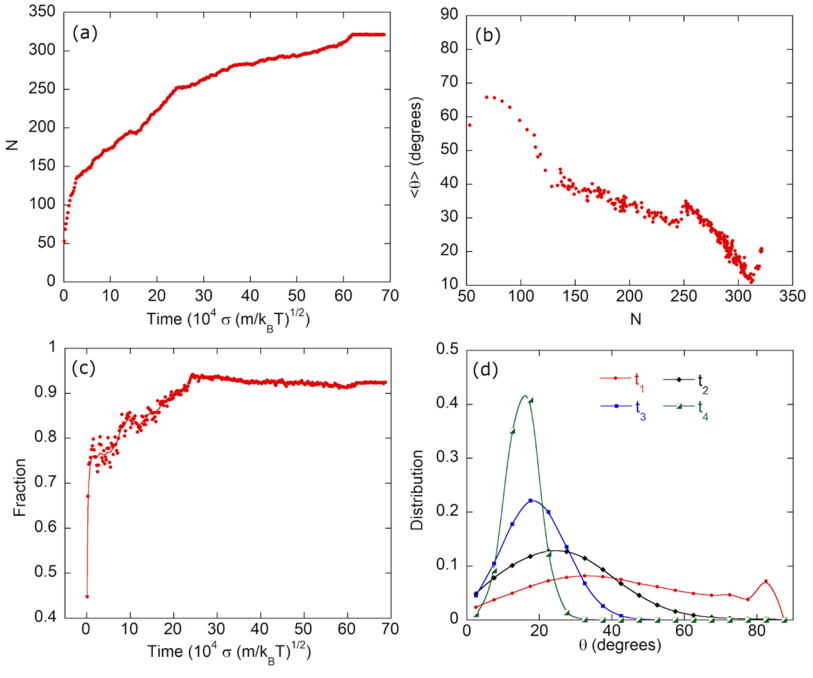

Figure 5. Results of a simulation trajectory with $(\varepsilon_{TS}, \varepsilon_{HS}) = (0.36, 5.0)$. In this trajectory, a SAM configuration is achieved via formation of islands of standing-up adsorbed molecules. (a) N as a function of time. (b) $\langle\theta\rangle$ as a function of N. (c) Fraction as a function of time. (d) Distribution of θ for different time periods ($t_4 > t_3 > t_2 > t_1$). Each time period spans $4.3 \times 10^4\, \sigma(m/k_BT)^{1/2}$ time. t_1 corresponds to the period when N varies from 40 to 140, t_2 corresponds to N from 205 to 235, t_3 corresponds to N from 280 to 290, and t_4 corresponds to N from 319 to 322.

formation of a partial second layer of adsorbed molecules. Figure 3b informs that, in the stripe configuration, the molecules stack up in nearly eight distinct molecular layers. Interestingly, the total numbers of adsorbed molecules in the SAM and the stripe configuration are similar, even when the adsorbed configurations are significantly different. This result suggests that adsorbed morphology cannot be conclusively deduced from the adsorbed amount alone.[24]

4.2. Kinetics of SAM Formation. As discussed above, experiments have revealed two different kinetic pathways leading to the formation of a SAM: in the first pathway, molecules initially adsorb lying down on the surface and that is followed by an orientational transition from the stripe to the

DOI: 10.1021/acs.jpcb.9b05861
J. Phys. Chem. B XXXX, XXX, XXX−XXX

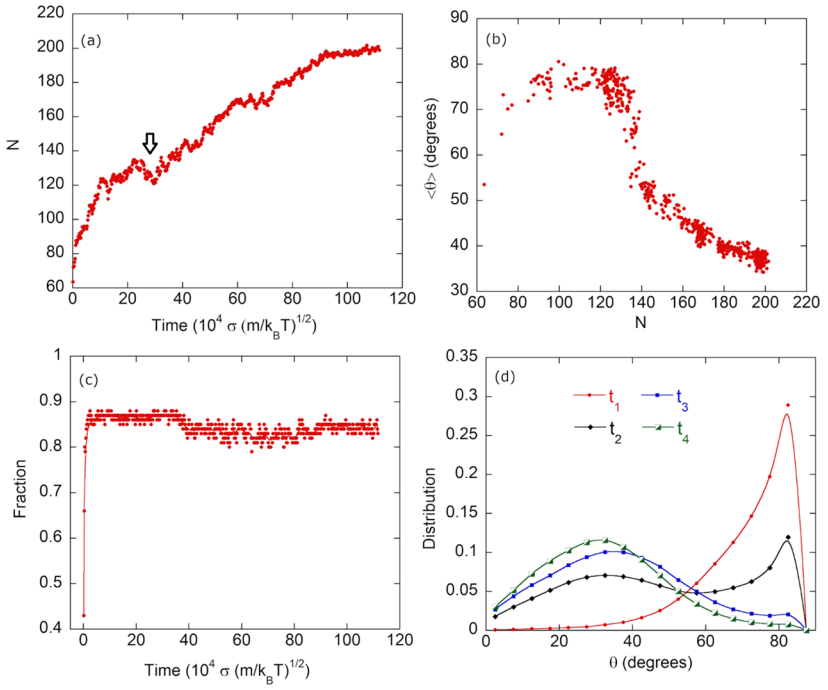

Figure 6. A simulation trajectory of 30-mer surfactant molecules with $(\varepsilon_{TS}, \varepsilon_{HS}) = (0.4, 4.0)$. (a) N as a function of time. (b) $\langle\theta\rangle$ as a function of N. (c) *Fraction* as a function of time. (d) Distribution of θ for different time periods ($t_4 > t_3 > t_2 > t_1$, see text).

SAM configuration. In the second pathway, islands of adsorbed molecules standing up on the surface form. These islands grow and coalesce to become a SAM. Both these kinetic pathways are observed in our simulations. The stripe-to-SAM orientational transition is observed when the $\frac{E^L}{E^S}$ is close to 1, roughly $0.8 < \frac{E^L}{E^S} < 1$. We illustrate this orientational transition by describing a simulation trajectory for the case $(\varepsilon_{TS}, \varepsilon_{HS}) = (0.49, 3.0)$ for which the $\frac{E^L}{E^S} = 0.9$ and it eventually forms a SAM (see Figure 1).

Movie S1 shows a movie of the simulation trajectory for $(\varepsilon_{TS}, \varepsilon_{HS}) = (0.49, 3.0)$ in which the stripe-to-SAM orientational transition is clearly seen. For this simulation trajectory, Figure 4a shows the total number of surfactant molecules adsorbed, N as a function of time. The initial adsorption is rapid followed by a more gradual adsorption. Figure 4b shows the average angle of the axes of the adsorbed molecules with the surface normal $\langle\theta\rangle$ as a function of N. During initial adsorption, the molecules lie flat on the surface as evidenced by $\langle\theta\rangle \approx 80°$. Beyond $N \sim 160$, a rapid decrease in the $\langle\theta\rangle$ is observed, indicating that the adsorbed molecules undergo an orientational transition and start standing up on the surface. The arrow in Figure 4a indicates the point in the trajectory when the stripe-to-SAM transition occurs. Figure 4c shows the fraction of the surface covered by the adsorbed molecules, *Fraction* as a function of time. Details of calculating *Fraction* are provided in the Supporting Information. It is observed that *Fraction* > 0.8 is reached in a much quicker time $(\sim 1 \times 10^4\ \sigma(m/k_BT)^{1/2})$ than the orientational transition $(\sim 20 \times 10^4\ \sigma(m/k_BT)^{1/2})$ indicating that the molecules in the stripe configuration cover the entire surface before undergoing the transition. Figure 4d shows the distribution of θ of adsorbed molecules at different time periods. Each time period spans $4.3 \times 10^4\ \sigma(m/k_BT)^{1/2}$. In the t_1 time period, N varies from 145 to 160; in the t_2 time period, N varies from ~182 to 190; in the t_3 time period, N varies from ~220 to 230; in the t_4 time period, N varies from ~288 to 292. In the t_1 period, the distribution of θ is predominantly around 80° indicating that the adsorbed molecules lie flat on the surface. The period t_2 shows initiation of the orientational transition with the peak around 80° becoming shallower and a bump appearing near 20°. In the period t_3, the peak in the distribution of θ is shifted to 20° indicating that the molecules now stand up on the surface. In the period t_4, the distribution of θ is sharper and the peak is shifted to 12°, which is the case when the entire surface is covered with a SAM of adsorbed molecules.

The second kinetic pathway, in which islands of molecules are formed that coalesce into a SAM, is observed when $\frac{E^L}{E^S} < 0.6$. Figure 5 shows details of such a simulation trajectory for $(\varepsilon_{TS}, \varepsilon_{HS}) = (0.36, 5.0)$. For this case, $\frac{E^L}{E^S} = 0.53$. The $\langle\theta\rangle$ is found to decrease with N indicating that the adsorbed molecules are standing up on the surface (Figure 5b). The *Fraction* saturates to 0.9 (complete coverage) much more sluggishly (only after $25 \times 10^4\ \sigma(m/k_BT)^{1/2}$ time steps) showing that there are islands of adsorbed molecules as well as a bare, exposed surface (Figure 5c). Figure 5d shows distributions of θ at different times. During the first time period t_1 where the N varies from 40 to 140, the distribution has a peak at 30°, indicating that the molecules are already standing up on the surface. The peak at these small values of θ becomes sharper as more adsorption occurs. Basically, when $E^L \ll E^S$, the molecules have a strong tendency to stand up in the adsorbed state, which leads to the formation of islands and a stripe configuration does not form.

Figure S1 shows a simulation trajectory for $(\varepsilon_{TS}, \varepsilon_{HS}) = (0.49, 2.0)$ for which the stripe configuration is achieved. Figure S2 shows a simulation trajectory for $(\varepsilon_{TS}, \varepsilon_{HS}) = (0.4, 2.5)$, which is another example of a stripe-to-SAM transition. Kindly see the Supporting Information for more details of these trajectories.

4.3. Validating the Theoretical Model for 30-Mer Surfactants. We have tested our theoretical model on 30

DOI: 10.1021/acs.jpcb.9b05861
J. Phys. Chem. B XXXX, XXX, XXX−XXX

bead long linear surfactant molecules by performing Langevin dynamics simulations for two state points (ε_{TS}, ε_{HS}) = (0.4, 4.0) and (ε_{TS}, ε_{HS}) = (0.5, 4.0). For this system, $\sigma = 1$, $d = 1$, and $l = 9$. Following the above strategy, we set $\varepsilon_{TT} = 0.046$, which has been shown to result in maximal adsorption when the tail−surface interactions are zero.[19] Figure 6 shows the kinetics of adsorption for (ε_{TS}, ε_{HS}) = (0.4, 4.0) wherein a SAM is formed. The adsorption is observed to be sluggish as compared to the 20-mer case (Figure 6a). The maximum adsorbed amount is $N \sim 200$, which corresponds to $P^S = 0.4$. From eq 3, $\frac{E^L}{E^S} = 0.87$ for (ε_{TS}, ε_{HS}) = (0.4, 4.0) suggesting that the preference is to form a SAM. For (ε_{TS}, ε_{HS}) = (0.5, 4.0), eq 3 gives $\frac{E^L}{E^S} = 1.03$, indicating that a stripe configuration should form, which is indeed the case (Figure S3). The N as a function of time is plotted in Figure 6a. The arrow indicates when the stripe-to-SAM orientational transition is observed. The stripe-to-SAM transition corresponds to a decrease in the $\langle\theta\rangle$ (Figure 6b). Figure 6c shows that the Fraction becomes greater than 0.8 within 1×10^4 $\sigma(m/k_BT)^{1/2}$ time, which is much earlier than the stripe-to-SAM transition time indicating that the stripe configuration occupies the entire adsorbing surface. The distribution of θ at different times during the adsorption is displayed in Figure 6d. The behavior of the distribution is similar to that in Figure 4d. At time t_1 (corresponding to $N \sim 110-122$), the distribution is peaked at ∼80°, which implies the presence of the stripe configuration. At t_2 ($N \sim 132-146$), there are peaks at ∼30° and ∼80° suggesting that the configuration is in the midst of the stripe-to-SAM transition. At times t_3 ($N \sim 166-176$) and t_4 ($N \sim 200$), the peak in the distribution is closer to 30° since a SAM configuration has formed. These results confirm the applicability of our theoretical model to surfactants of different alkyl tail lengths.

4.4. Conditions for Validity of our Theoretical Model.

We have provided a theoretical framework to predict equilibrium adsorbed configurations of linear surfactant molecules on polar surfaces. Our theory only considers energetic terms but ignores entropic changes during adsorption. Therefore, we would expect this theory to be valid for cases where significant adsorption, resulting in complete surface coverage, is observed. In cases of partial adsorption, a balance of the entropic and energetic terms between the bulk and adsorbed states is expected to exist, and our theory will fail to explain these scenarios. Furthermore, even though tail−tail interactions do not enter in our equations, our theory is expected to be applicable for cases where these interactions are significant so that stable SAM and stripe configurations are formed. While these conditions are the limits on the applicability of our theory, it still encompasses a large number of systems of interest, such as surfactants adsorbing on metal and polar surfaces in aqueous media.

In this work, the theoretical model is validated by performing implicit solvent Langevin dynamics simulations of a coarse-grained model of surfactant molecules. This system was selected because of its computational efficiency, which allowed us to sample numerous data points that were needed for proper validation of the model. Even with this coarse-grained description, the self-assembly of surfactants in organized layers was found to be a slow process, as can be seen from the kinetic results. Explicit treatment of water will have an effect on the adsorption behavior. Water adsorbs in layers on metal and polar surfaces and solvates polar heads of the surfactants.[23] As a result, along with direct interactions between the surfactants and the surface, there will be indirect, water-mediated interactions as well. For applying our theoretical model to a fully atomistic simulation, we will need to include these interactions by calculating the potential of mean force between different species. Furthermore, the presence of water may present free energy barriers to adsorption,[23] which may affect the diffusion of surfactants toward the surface. The application of our theoretical model on a fully atomistic system will be a subject of future research.

5. CONCLUSIONS

We have developed a theoretical model for predicting adsorbed configurations of linear surfactant molecules on polar surfaces. We have validated the predictions of the model by performing Langevin dynamics simulations. The model also shows that the ratio of energies associated with the lying down and standing-up configurations, $\frac{E^L}{E^S}$ is a good indicator for predicting the kinetic pathway associated with SAM formation. In future work, we will extend and test the predictions of this model for different surfactant geometries and anisotropic interactions.

■ ASSOCIATED CONTENT

Supporting Information

The Supporting Information is available free of charge on the ACS Publications website at DOI: 10.1021/acs.jpcb.9b05861.

Details of calculation of *Fraction* are discussed; following simulation trajectories are discussed: (ε_{TS}, ε_{HS}) = (0.49, 2.0), (ε_{TS}, ε_{HS}) = (0.4, 2.5), and (ε_{TS}, ε_{HS}) = (0.5, 4.0) for 30-mer surfactants (PDF)

A movie of the simulation trajectory with (ε_{TS}, ε_{HS}) = (0.49, 3.0) (MPG)

■ AUTHOR INFORMATION

Corresponding Author

*E-mail: sharmas@ohio.edu.

ORCID

Sumit Sharma: 0000-0003-3138-5487

Xueying Ko: 0000-0002-7744-7690

Notes

The authors declare no competing financial interest.

■ ACKNOWLEDGMENTS

This work is supported by the NSF CBET grant 1705817. The authors thank researchers at the Institute for Corrosion and Multiphase Technology (ICMT) for useful discussions. X.K. thanks the support of Ohio University Graduate College Fellowship for the year 2018−2019. S.S. thanks Ohio University for covering computational costs for resources provided by the Ohio Supercomputer Center. S.S. thanks additional computational resources from National Science Foundation XSEDE grant number DMR190005.

■ REFERENCES

(1) Edwards, A.; Osborne, C.; Webster, S.; Klenerman, D.; Joseph, M.; Ostovar, P.; Doyle, M. Mechanistic Studies of the Corrosion Inhibitor Oleic Imidazoline. *Corros. Sci.* **1994**, *36*, 315−325.

(2) Li, J.; Kaifer, A. E. Surfactant Monolayers on Electrode Surfaces: Self-Assembly of a Viologen Derivative Having a Cholesteryl Hydrophobic Residue. *Langmuir* **1993**, *9*, 591−596.

DOI: 10.1021/acs.jpcb.9b05861
J. Phys. Chem. B XXXX, XXX, XXX−XXX

(3) Murphy, C. J.; Sau, T. K.; Gole, A. M.; Orendorff, C. J.; Gao, J.; Gou, L.; Hunyadi, S. E.; Li, T. Anisotropic Metal Nanoparticles: Synthesis, Assembly, and Optical Applications. *J. Phys. Chem. B* **2005**, *109*, 13857−13870.
(4) Marshall, S. T.; O'Brien, M.; Oetter, B.; Corpuz, A.; Richards, R. M.; Schwartz, D. K.; Medlin, J. W. Controlled Selectivity for Palladium Catalysts Using Self-Assembled Monolayers. *Nat. Mater.* **2010**, *9*, 853.
(5) Manne, S.; Cleveland, J. P.; Gaub, H. E.; Stucky, G. D.; Hansma, P. K. Direct Visualization of Surfactant Hemimicelles by Force Microscopy of the Electrical Double Layer. *Langmuir* **1994**, *10*, 4409−4413.
(6) Manne, S.; Gaub, H. E. Molecular Organization of Surfactants at Solid-Liquid Interfaces. *Science* **1995**, *270*, 1480−1482.
(7) Qi, X.; Balankura, T.; Zhou, Y.; Fichthorn, K. A. How Structure-Directing Agents Control Nanocrystal Shape: Polyvinylpyrrolidone-mediated Growth of Ag Nanocubes. *Nano Lett.* **2015**, *15*, 7711−7717.
(8) Schoenbaum, C. A.; Schwartz, D. K.; Medlin, J. W. Controlling the Surface Environment of Heterogeneous Catalysts Using Self-Assembled Monolayers. *Acc. Chem. Res.* **2014**, *47*, 1438−1445.
(9) Johnson, R. A.; Nagarajan, R. Modeling Self-Assembly of Surfactants at Solid/Liquid Interfaces. I. Hydrophobic Surfaces. *Colloids Surf., A* **2000**, *167*, 31−46.
(10) Johnson, R. A.; Nagarajan, R. Modeling Self-Assembly of Surfactants at Solid−Liquid Interfaces. II. Hydrophilic Surfaces. *Colloids Surf., A* **2000**, *167*, 21−30.
(11) Xu, S.-L.; Wang, C.; Zeng, Q.-D.; Wu, P.; Wang, Z.-G.; Yan, H.-K.; Bai, C.-L. Self-Assembly of Cationic Surfactants on a Graphite Surface Studied by STM. *Langmuir* **2002**, *18*, 657−660.
(12) Jaschke, M.; Butt, H.-J.; Gaub, H. E.; Manne, S. Surfactant Aggregates at a Metal Surface. *Langmuir* **1997**, *13*, 1381−1384.
(13) Hayes, W. A.; Schwartz, D. K. Two-Stage Growth of Octadecyltrimethylammonium Bromide Monolayers at Mica from Aqueous Solution Below the Krafft Point. *Langmuir* **1998**, *14*, 5913−5917.
(14) Shimazu, K.; Yagi, I.; Sato, Y.; Uosaki, K. In Situ and Dynamic Monitoring of the Self-Assembling and Redox Processes of a Ferrocenylundecanethiol Monolayer by Electrochemical Quartz Crystal Microbalance. *Langmuir* **1992**, *8*, 1385−1387.
(15) Woodward, J. T.; Doudevski, I.; Sikes, H. D.; Schwartz, D. K. Kinetics of Self-Assembled Monolayer Growth Explored via Sub-monolayer Coverage of Incomplete Films. *J. Phys. Chem. B* **1997**, *101*, 7535−7541.
(16) Doudevski, I.; Hayes, W. A.; Schwartz, D. K. Submonolayer Island Nucleation and Growth Kinetics During Self-Assembled Monolayer Formation. *Phys. Rev. Lett.* **1998**, *81*, 4927.
(17) Poirier, G. E.; Pylant, E. D. The Self-Assembly Mechanism of Alkanethiols on Au (111). *Science* **1996**, *272*, 1145−1148.
(18) Xu, S.; Cruchon-Dupeyrat, S. J. N.; Garno, J. C.; Liu, G.-Y.; Kane Jennings, G.; Yong, T.-H.; Laibinis, P. E. In situstudies of Thiol Self-Assembly on Gold from Solution Using Atomic Force Microscopy. *J. Chem. Phys.* **1998**, *108*, 5002−5012.
(19) Ko, X.; Sharma, S. Adsorption and Self-Assembly of Surfactants on Metal−Water Interfaces. *J. Phys. Chem. B* **2017**, *121*, 10364−10370.
(20) Allen, M. P.; Tildesley, D. J. *Computer Simulation of Liquids*; Oxford University Press: Oxford, U.K., 1989.
(21) Choudhury, N.; Pettitt, B. M. On the Mechanism of Hydrophobic Association of Nanoscopic Solutes. *J. Am. Chem. Soc.* **2005**, *127*, 3556−3567.
(22) Kovačević, N.; Milošev, I.; Kokalj, A. How Relevant is the Adsorption Bonding of Imidazoles and Triazoles for their Corrosion Inhibition of Copper? *Corros. Sci.* **2017**, 25.
(23) Kurapati, Y.; Sharma, S. Adsorption Free Energies of Imidazolinium-Type Surfactants in Infinite Dilution and in Micellar State on Gold Surface. *J. Phys. Chem. B* **2018**, *122*, 5933−5939.
(24) McMahon, A. J. The Mechanism of Action of an Oleic Imidazoline Based Corrosion Inhibitor for Oilfield Use. *Colloids Surf.* **1991**, *59*, 187−208.

DOI: 10.1021/acs.jpcb.9b05861
J. Phys. Chem. B XXXX, XXX, XXX−XXX